

Cobalt-Catalyzed Reductive C–O Bond Cleavage of Lignin β -O-4 Ketone Models via In Situ Generation of the Cobalt–Boryl Species

Kecheng Gao,[†] Man Xu,[†] Cheng Cai, Yanghao Ding, Jianhui Chen,^{*} Bosheng Liu, and Yuanzhi Xia^{*}

Cite This: <https://dx.doi.org/10.1021/acs.orglett.0c02117>

Read Online

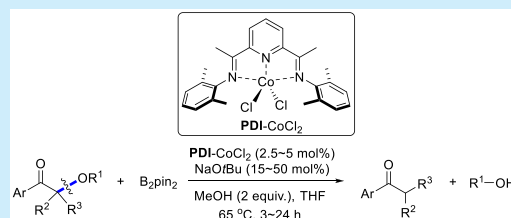
ACCESS |

Metrics & More

Article Recommendations

Supporting Information

ABSTRACT: An efficient and mild method for reductive C–O bond cleavage of lignin β -O-4 ketone models was developed to afford the corresponding ketones and phenols with PDI-CoCl₂ as the precatalyst and diboron reagent as the reductant. The synthetic utility of the methodology was demonstrated by depolymerization of a polymeric model and gram-scale transformation. Mechanistic studies suggested that this transformation involves steps of carbonyl insertion, 1,2-Brook type rearrangement, β -oxygen elimination, and rate-limiting regeneration of the catalytic active Co–B species.

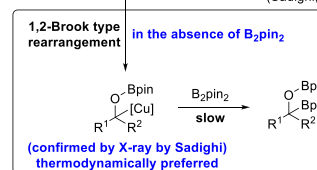
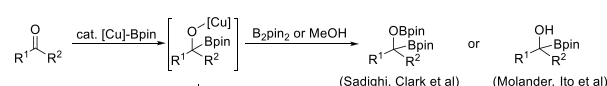


Lignin is a class of important aromatic biopolymers and represents ~30% of nonfossil organic carbon.¹ Thus, degradation of lignin is a sustainable way to produce bulk chemicals, which has attracted a great deal of attention in both academia and industry.² The primary structure of lignin consists of electron-rich phenyl propanol units randomly joined by many different linkages, in which the β -O-4 unit is the most abundant.³ A variety of elegant strategies, including oxidative,⁴ reductive,⁵ and redox-neutral⁶ protocols, have been developed to cleave the β -O-4 linkages in recent years. However, due to its high bond energy and complex structure consisting of C–C and C–O linkages,⁷ these methods generally suffered from high temperatures, low yields, and low chemoselectivity. Hence, the development of an efficient and mild strategy for selective cleavage of β -O-4 linkages is highly valuable.

In the past two decades, an increasing level of attention has been paid to the earth-abundant transition metal–boryl (M–B) complexes generated in situ from a mixture of metal salt, diboron reagent, and base,⁸ as these species have been found to be catalytically active for various important transformations.⁹ In 2006, Sadighi and co-workers pioneered the catalytic diboration of aldehydes, which was mediated via insertion of an aldehyde C=O group into a Cu–B bond process (Scheme 1a).^{10,11} Subsequently, Lin and Marder investigated the detailed mechanism with the aid of DFT calculations,¹² showing that the intermediate from carbonyl insertion having a Cu–O–C–B linkage would convert to the thermodynamically preferred Cu–C–O–B isomer via 1,2-Brook type rearrangement^{13,14} in the absence of a diboron reagent. In 2012, Molander et al. applied this methodology to monoboration of aldehydes with MeOH as a proton source.¹⁵ Recently, Ito and co-workers developed an asymmetric version of copper-catalyzed monoboration of aldehydes and ketones, producing chiral alcohol derivatives efficiently.¹⁶ To the best of our knowledge, the application of metal–boryl catalysis for C–O

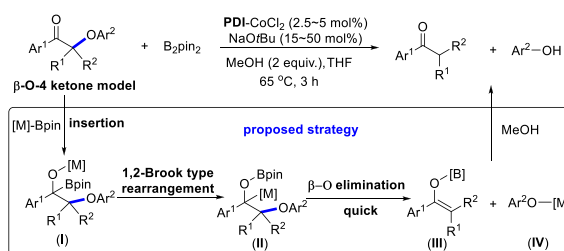
Scheme 1. Catalytic Transformations Mediated via Insertion of a C=O Group into the M–B Bond

(a) Cu-catalyzed di- and monoborylation of aldehydes or ketones (previous work):



DFT studies by Lin and Marder

(b) Co-catalyzed C–O bond cleavage of β -O-4 ketone models (this work):



bond cleavage of β -O-4 linkages has not been reported so far. We postulated that beginning with the insertion of a C=O group into the M–B bond to generate a M–O–C–B species (I) and the subsequent 1,2-Brook type rearrangement to form

Received: June 29, 2020

the thermodynamically preferred M–C–O–B species (II), the M–B catalysis could serve as a platform for C–O bond cleavage of lignin β -O-4 ketone models by β -O elimination¹⁷ (Scheme 1b). This approach affords alkenyl boron ether (III) and phenoxyl-metal (IV) and finally generates the corresponding ketone and phenol as the products by protonation.

Our investigation began with the evaluation of reaction parameters using 2-phenoxy-1-phenylethan-1-one (1a) as the model substrate (Table 1). After screening the reaction

Table 1. Optimization of Reaction Conditions

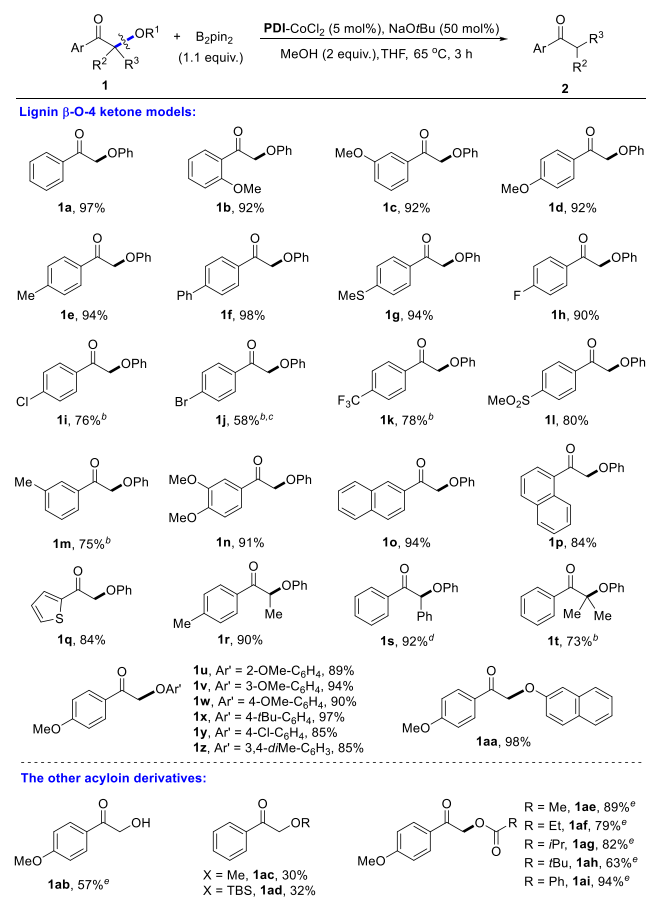
entry	deviation from standard conditions ^a	2a (%) ^b
1	none	99 (97) ^c
2	PDI with NiCl ₂ instead of PDI-CoCl ₂	78
3	PDI with CuCl ₂ instead of PDI-CoCl ₂	15
4	PDI with CuCl instead of PDI-CoCl ₂	23
5	PDI with MnCl ₂ instead of PDI-CoCl ₂	8
6	PDI with FeCl ₂ instead of PDI-CoCl ₂	32
7	PDI with ZnCl ₂ instead of PDI-CoCl ₂	5
8	OIP-CoCl ₂ instead of PDI-CoCl ₂	60
9	PAO with CoCl ₂ instead of PDI-CoCl ₂	56
10	PNP with CoCl ₂ instead of PDI-CoCl ₂	32
11	Xantphos with CoCl ₂ instead of PDI-CoCl ₂	18
12	with 10 mol % NaOtBu	80–94
13	no PDI-CoCl ₂	9
14	no MeOH	57
15	no NaOtBu	trace
16	at 25 °C	73

^aThe reaction was conducted with 1a (0.5 mmol), PDI-CoCl₂ (0.025 mmol), B₂pin₂ (0.55 mmol), NaOtBu (0.25 mmol), and MeOH (1 mmol) in THF (1 mL) at 65 °C for 3 h. ^bYields were determined by ¹H NMR using mesitylene as the internal standard. ^cIsolated yield.

conditions, we found 1a could exclusively convert to acetophenone (2a) in the presence of B₂pin₂ (1.1 equiv) at 65 °C when PDI-CoCl₂, NaOtBu, MeOH, and THF were used as the catalyst, base, additive, and solvent, respectively (entry 1). The nickel complex also acted as a competent catalyst for this transformation (entry 2). Employing another earth-abundant transition metal catalyst (Cu, Mn, Fe, or Zn), the desired product 2a was formed in poor yields (entries 3–7). The combinations of CoCl₂ with other ligands were also tested, giving 2a in 32–60% yields (entries 8–11). When the load of NaOtBu was decreased to 10 mol %, the reaction could also proceed smoothly to give 2a in good yield (entry 12). However, the yield was unstable, because the NaOtBu powder would adhere to the inner wall of the tube during its addition. Control experiments established that the metal catalyst, base, and MeOH were essential for the excellent yield of 2a (entries 13–15, respectively). However, employing reducing agents, including NaHBET₃ and KC₈, instead of a base also made this reaction feasible (Table S1). In addition, decreasing the temperature to 25 °C led to a relatively lower yield of 2a (entry 16).

With the optimized reaction conditions in hand, the substrate scope was next expanded (Scheme 2). The position

Scheme 2. Substrate Scope^a



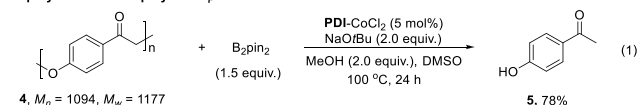
^aThe reaction was conducted with 1 (0.50 mmol), B₂pin₂ (0.55 mmol), PDI-CoCl₂ (0.025 mmol), NaOtBu (0.25 mmol), and MeOH (1.0 mmol) in THF (1 mL) at 65 °C for 3 h. ^bTwelve hours. ^cAccompanied by ~5 mol % dehalogenated product. ^dB₂pin₂ (1.0 mmol) for 24 h. ^eB₂pin₂ (0.75 mmol) and NaOtBu (0.50 mmol) for 24 h.

of the substituent on the phenyl ring (Ar) did not alter the reaction efficiency as demonstrated with the methoxy substituent (1b–1d). The substituents of alkyl, phenyl, protected thiophenol, and fluoro at the *para* position of the phenyl ring could be well tolerated (1e–1h, respectively). The reactions of substrates containing chloro and bromo atoms gave the products in slightly lower yields (1i and 1j, respectively), and ~5% of the dehalogenated product formed in the reaction of 1j. Strongly electron-deficient substituents such as trifluoromethyl (1k) and methylsulfonyl (1l) group were compatible with this catalytic system. A substrate bearing two substituents on the phenyl ring resulted in a similar reaction activity (1n). Other aryl rings such as 2-naphthalene, 1-naphthalene, and thiophene were well tolerated to afford the desired products in 84–94% yields (1o–1q, respectively). Secondary alcohol derivatives (1r and 1s) facilitated this transformation and delivered the corresponding ketones in excellent yields. In addition, deoxygenation of the tertiary alcohol derivative (1t) afforded 2t in 73% yield. Different R¹ groups were then investigated (1u–1ag). The steric and

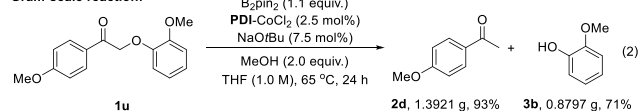
electronic effect of substituents on the aryl ring (R^1) had a marginal influence on the yield (**1u–1aa**). A direct cleavage of the free hydroxyl group was also achieved employing this catalytic system (**1ab**). The reactions of substrates with OMe and OTBS as the leaving groups were much less efficient (**1ac** and **1ad**). In the case of substrates bearing α -acyl groups, the catalytic system afforded the deoxygenation products efficiently (**1ae–1ai**), albeit a relatively longer reaction time was required for these cases.

To further showcase the synthetic utility, the catalytic system was applied to depolymerization of a polymeric lignin β -O-4 ketone model (**4**), producing the ketone monomer (**5**) in 78% yield (eq 1). The C–O bond cleavage reaction could be scaled up to gram scale smoothly, affording the corresponding ketone and phenol in 93% and 71% yields, respectively (eq 2).

Depolymerization of polymeric β -O-4 ketone model:



Gram-scale reaction:



To explore the mechanistic details of this transformation, we conducted quantitative kinetic studies (Figure 1) to determine

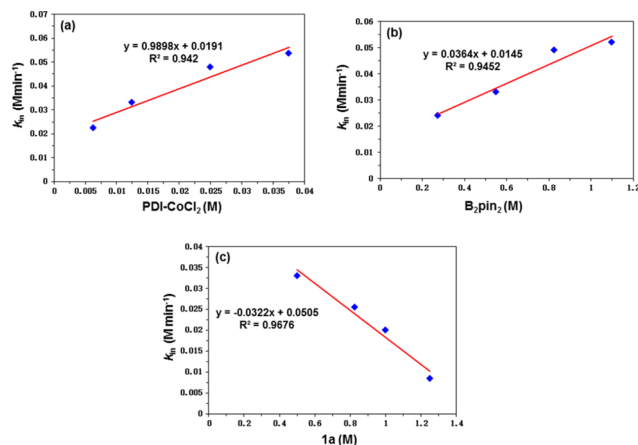
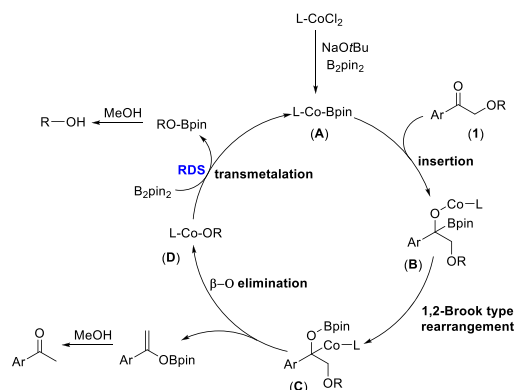


Figure 1. Quantitative kinetic studies. (a) Plot of k_{in} vs $PDI-CoCl_2$ concentration. (b) Plot of k_{in} vs B_2pin_2 concentration. (c) Plot of k_{in} vs **1a** concentration.

the role of the substrate (**1a**), B_2pin_2 , and catalyst at the rate-determining step (RDS). Measurements of the initial rates (k_{in}) for the reaction of **1a** with different concentrations of $PDI-CoCl_2$ and B_2pin_2 showed increases in the rates. Plots of k_{in} versus the concentration of $PDI-CoCl_2$ (Figure 1a) and B_2pin_2 (Figure 1b) gave two linear curves (slopes of 1.91×10^{-2} and $1.45 \times 10^{-2} M \cdot min^{-1}$, respectively), which suggested a first-order rate dependence on catalyst and B_2pin_2 . However, an inverse correlation was found between k_{in} and the concentration of **1a** (Figure 1c). These quantitative kinetic studies indicated that B_2pin_2 should be involved in the RDS and the reaction is slowed by excess substrate **1a**.

On the basis of the quantitative kinetic studies and literature report¹² on insertion of a C=O group into the Cu–B bond, a plausible catalytic cycle is proposed in Scheme 3. First, a

Scheme 3. Proposed Mechanism



ligated cobalt–boryl species (**A**) is generated by treating the $PDI-CoCl_2$ complex with a base and B_2pin_2 .^{8d,18,19} Following the coordination of the substrate to the cobalt center, insertion of a C=O group into the Co–B bond forms species **B**, which undergoes 1,2-Brook type rearrangement to produce species **C**. Then, β -O elimination yields alkenyl boron ether and cobalt-alkoxy species (**D**).²⁰ Finally, regeneration of **A** occurs via a rate-limiting transmetalation process between **D** and B_2pin_2 .

DFT calculations were carried out to improve our understanding (Figures 2 and 3). Upon the formation of Co(I)–boryl species **A**,^{8d} its complexation with **1a** to form **IN1** is almost energetically neutral (Figure 2). The insertion of the carbonyl functionality of **1a** into the Co–B bond of **A** occurs via **TS1** readily with an activation barrier of 10.1 kcal/mol, giving rise to intermediate **IN2** exergonically. The energy for regioisomeric insertion is much higher than that for **TS1** (Figure S5). To undergo further transformation, the 1,2-Brook type rearrangement would occur first to generate the alkyl Co species. This process is realized via a stepwise reaction by the generation of a three-membered ring intermediate **IN3** via **TS2**, requiring a barrier of only 6.5 kcal/mol and being slightly endergonic. From zwitterionic species **IN3**, C–B bond cleavage via **TS3** is very easy and leads exergonically to alkyl Co(I) complex **IN4** in which the Co atom is associated strongly with the O atom with a Co–O distance of 2.08 Å. The dissociation of the Co–O interaction is favorable as **IN5** would be much lower in energy than **IN4**. Prior to the β -oxygen elimination, complex **IN6**, in which the phenoxide oxygen is associated with the Co, should be formed from **IN5** by bond rotation. From **IN6**, C–O bond cleavage occurs via **TS4** with a barrier of 12.2 kcal/mol, leading to alkenyl boron ether **IN7** and Co(I)-phenoxide highly exergonically. The final product could be formed by further protonation of **IN7**.

The regeneration of catalytic species **A** from the Co(I)-phenoxide ($LCO-OPh$) was next investigated. The direct metathesis of $LCO-OPh$ with B_2pin_2 involves two steps (Figure 3a). The first step is phenoxide transfer. In this step, the Co–O bond is cleaved via **TS5**, from which the phenoxide moiety is transferred to the boron moiety with a barrier of 22.7 kcal/mol to form zwitterionic intermediate **IN8** exergonically. In **IN8**, the B1–O distance is obviously longer than the normal B–O bond (1.60 Å in **IN8** vs 1.36 Å in **IN11**) while the B1–B2 distance is almost unchanged (1.76 Å in **IN8** vs 1.71 Å in B_2pin_2). Prior to the second step of boryl transfer, **IN8** should first isomerize to **IN9**. In the latter complex, the negative charge on B2 is stabilized by both Co (Co–B2 = 2.35 Å) and B1 (B1–B2 = 1.89 Å) and the B1–O interaction is enhanced

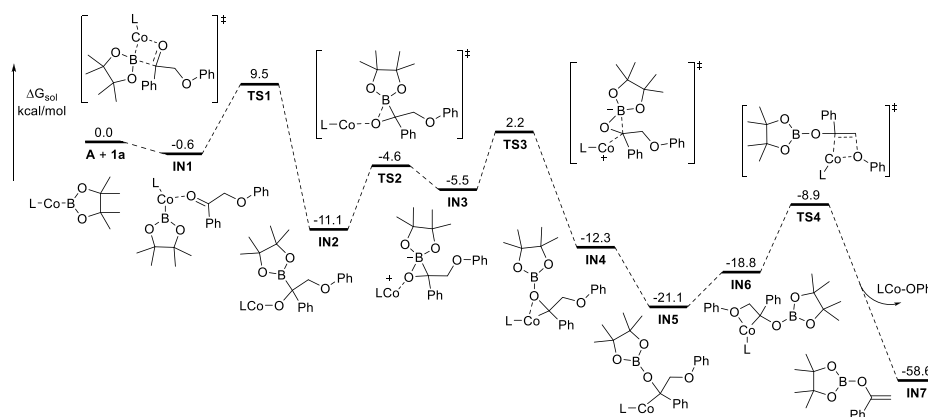


Figure 2. DFT-calculated energy profile for the generation of alkenyl boron ether IN7 starting from A and 1a (L = PDI).

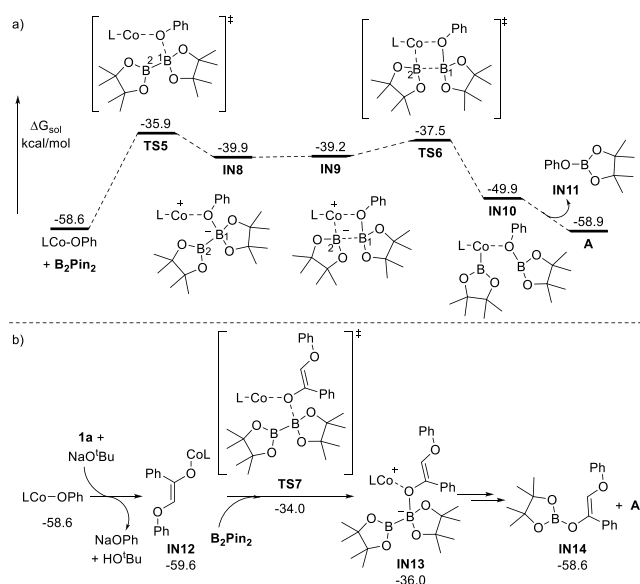


Figure 3. DFT-calculated energy profile for the regeneration of active species A (L = PDI).

(B1–O = 1.52 Å). IN9 is unstable and undergoes the boryl transfer readily via TS6, from which the B1–B2 is completely destroyed and the complex IN10 is formed. Finally, A is regenerated by dissociation of IN11 from Co. Accordingly, the transfer of the phenoxide moiety to B₂Pin₂ via TS5 is the most difficult step, in good agreement with the kinetic results.

The observed inverse correlation of the reaction rate and concentration of 1a from quantitative kinetic studies could be probably attributed to more difficult metathesis if LCo–OPh reacts first with 1a (Figure 3b). In the presence of excess 1a and NaOtBu, the transformation of Co(I)-phenoxide to Co(I)-enolate IN12 would be energetically favored by 1.0 kcal/mol. From the latter intermediate, the enolate transfer from Co to B via TS7 requires an activation barrier of 25.6 kcal/mol. The generated zwitterionic species IN13 will finally deliver A and IN14 by boryl transfer. Thus, the barrier required for metathesis involving enolate would be at least 2.9 kcal/mol higher than that shown in Figure 3a, being in qualitative agreement with the experimental observation.

In summary, we have developed an efficient method for reductive C–O bond cleavage with a cobalt catalyst in the presence of a diboron reagent and base, converting lignin β-O-

4 ketone models into the corresponding ketones and phenols. This reaction could be applied to depolymerization of polymeric lignin β-O-4 ketone and scaled up to gram scale smoothly. Mechanistic investigations by quantitative kinetic studies and DFT calculations indicated the in situ-generated cobalt–boryl complex is the catalytically active species and the 1,2-Brook type rearrangement is involved in the generation of the alkyl-cobalt intermediate, from which the C–O bond cleavage occurs via β-O elimination.

ASSOCIATED CONTENT

Supporting Information

The Supporting Information is available free of charge at <https://pubs.acs.org/doi/10.1021/acs.orglett.0c02117>.

Experimental and computational details, data, and spectra (PDF)

AUTHOR INFORMATION

Corresponding Authors

Jianhui Chen – College of Chemistry and Materials Engineering, Wenzhou University, Wenzhou 325035, China; orcid.org/0000-0002-5080-1880; Email: cjh@wzu.edu.cn

Yuanzhi Xia – College of Chemistry and Materials Engineering, Wenzhou University, Wenzhou 325035, China; orcid.org/0000-0003-2459-3296; Email: xyz@wzu.edu.cn

Authors

Kecheng Gao – College of Chemistry and Materials Engineering, Wenzhou University, Wenzhou 325035, China

Man Xu – College of Chemistry and Materials Engineering, Wenzhou University, Wenzhou 325035, China

Cheng Cai – College of Chemistry and Materials Engineering, Wenzhou University, Wenzhou 325035, China

Yanghao Ding – College of Chemistry and Materials Engineering, Wenzhou University, Wenzhou 325035, China

Bosheng Liu – College of Chemistry and Materials Engineering, Wenzhou University, Wenzhou 325035, China

Complete contact information is available at: <https://pubs.acs.org/10.1021/acs.orglett.0c02117>

Author Contributions

†K.G. and M.X. contributed equally to this work.

Notes

The authors declare no competing financial interest.

ACKNOWLEDGMENTS

Financial support was provided by NSFC (21801191, 21572163, and 21873074), the Wenzhou Science & Technology Bureau (G20180016), the College Students Innovation and Entrepreneurship Training Program (JWSC2019060), and the Laboratory open project (JW20SK26) of Wenzhou University.

REFERENCES

- (1) Boerjan, W.; Ralph, J.; Baucher, M. LIGNIN BIOSYNTHESIS. *Annu. Rev. Plant Biol.* **2003**, *54*, 519–546.
- (2) For selected reviews, see: (a) Zakzeski, J.; Bruijninx, P. C. A.; Jongerijs, A. L.; Weckhuysen, B. M. The Catalytic Valorization of Lignin for the Production of Renewable Chemicals. *Chem. Rev.* **2010**, *110*, 3552–3599. (b) Li, C.; Zhao, X.; Wang, A.; Huber, G. W.; Zhang, T. Catalytic Transformation of Lignin for the Production of Chemicals and Fuels. *Chem. Rev.* **2015**, *115*, 11559–11624. (c) Rinaldi, R.; Jastrzebski, R.; Clough, M. T.; Ralph, J.; Kennema, M.; Bruijninx, P. C. A.; Weckhuysen, B. M. Paving the Way for Lignin Valorisation: Recent Advances in Bioengineering, Biorefining and Catalysis. *Angew. Chem., Int. Ed.* **2016**, *55*, 8164–8215. (d) Deuss, P. J.; Barta, K. From models to lignin: Transition metal catalysis for selective bond cleavage reactions. *Coord. Chem. Rev.* **2016**, *306*, 510–532. (e) Sun, Z.; Fridrich, B.; de Santi, A.; Elangovan, S.; Barta, K. Bright Side of Lignin Depolymerization: Toward New Platform Chemicals. *Chem. Rev.* **2018**, *118*, 614–678. (f) Das, A.; König, B. Transition metal- and photoredox-catalyzed valorisation of lignin subunits. *Green Chem.* **2018**, *20*, 4844–4852. (g) Van den Bosch, S.; Koelewijn, S.-F.; Renders, T.; Van den Bossche, G.; Vangeel, T.; Schutyser, W.; Sels, B. F. Catalytic Strategies Towards Lignin-Derived Chemicals. *Top. Curr. Chem.* **2018**, *376*, 36. (h) Liu, C.; Wu, S.; Zhang, H.; Xiao, R. Catalytic oxidation of lignin to valuable biomass-based platform chemicals: A review. *Fuel Process. Technol.* **2019**, *191*, 181–201.
- (3) Ralph, J.; Landucci, L. L. In *Lignin and Lignans: Advances in Chemistry*; Heitner, C., Dimmel, D., Schmidt, J., Eds.; CRC Press: Boca Raton, FL, 2010; pp 137–243.
- (4) For selected examples, see: (a) Sedai, B.; Díaz-Urrutia, C.; Baker, R. T.; Wu, R.; Silks, L. A.; Hanson, S. K. Aerobic oxidation of β -1 lignin model compounds with copper and oxovanadium catalysts. *ACS Catal.* **2013**, *3*, 3111–3122. (b) Wang, M.; Li, L. H.; Lu, J. M.; Li, H. J.; Zhang, X. C.; Liu, H. F.; Luo, N. C.; Wang, F. Acid promoted C–C bond oxidative cleavage of β -O-4 and β -1 lignin models to esters over a copper catalyst. *Green Chem.* **2017**, *19*, 702–706. (c) Zhu, C.; Ding, W.; Shen, T.; Tang, C.; Sun, C.; Xu, S.; Chen, Y.; Wu, J.; Ying, H. Metallo-deuteroporphyrin as a biomimetic catalyst for the catalytic oxidation of lignin to aromatics. *ChemSusChem* **2015**, *8*, 1768–1778. (d) Reichert, E.; Wintringer, R.; Volmer, D. A.; Hempelmann, R. Electro-catalytic oxidative cleavage of lignin in a protic ionic liquid. *Phys. Chem. Chem. Phys.* **2012**, *14*, 5214–5221.
- (5) For selected examples, see: (a) Galkin, M. V.; Samec, J. S. M. Selective route to 2-propenyl aryls directly from wood by a tandem organosolv and palladium-catalyzed transfer hydrogenolysis. *ChemSusChem* **2014**, *7*, 2154–2158. (b) Sergeev, A. G.; Hartwig, J. F. Selective, nickel-catalyzed hydrogenolysis of aryl ethers. *Science* **2011**, *332*, 439–443. (c) Nguyen, B. H.; Perkins, R. J.; Smith, J. A.; Moeller, K. D. Solvolysis, electrochemistry, and development of synthetic building blocks from sawdust. *J. Org. Chem.* **2015**, *80*, 11953–11962.
- (6) For selected examples, see: (a) Rahimi, A.; Azarpira, A.; Kim, H.; Ralph, J.; Stahl, S. S. Chemoselective Metal-Free Aerobic Alcohol Oxidation in Lignin. *J. Am. Chem. Soc.* **2013**, *135*, 6415–6418. (b) Galkin, M. V.; Sawadjoon, S.; Rohde, V.; Dawange, M.; Samec, J. S. M. Mild heterogeneous palladium-catalyzed cleavage of β -O-4'-ether linkages of lignin model compounds and native lignin in air. *ChemCatChem* **2014**, *6*, 179–184. (c) Nguyen, J. D.; Matsuura, B. S.; Stephenson, C. R. J. A Photochemical Strategy for Lignin Degradation at Room Temperature. *J. Am. Chem. Soc.* **2014**, *136*, 1218–1221. (d) Lancefield, C. S.; Ojo, O. S.; Tran, F.; Westwood, N. J. Isolation of functionalized phenolic monomers through selective oxidation and C–O bond cleavage of the β -O-4 linkages in lignin. *Angew. Chem., Int. Ed.* **2015**, *54*, 258–262. (e) Luo, N.; Wang, M.; Li, H.; Zhang, J.; Liu, H.; Wang, F. Photocatalytic Oxidation–Hydrogenolysis of Lignin β -O-4 Models via a Dual Light Wavelength Switching Strategy. *ACS Catal.* **2016**, *6*, 7716–7721. (f) Bosque, I.; Magallanes, G.; Rigoulet, M.; Kärkäs, M. D.; Stephenson, C. R. J. Redox Catalysis Facilitates Lignin Depolymerization. *ACS Cent. Sci.* **2017**, *3*, 621–628. (g) Magallanes, G.; Kärkäs, M. D.; Bosque, I.; Lee, S.; Maldonado, S.; Stephenson, C. R. J. Selective C–O Bond Cleavage of Lignin Systems and Polymers Enabled by Sequential Palladium-Catalyzed Aerobic Oxidation and Visible-Light Photoredox Catalysis. *ACS Catal.* **2019**, *9*, 2252–2260.
- (7) Kim, S.; Chmely, S. C.; Nimlos, M. R.; Bomble, Y. J.; Foust, T. D.; Paton, R. S.; Beckham, G. T. Computational Study of Bond Dissociation Enthalpies for a Large Range of Native and Modified Lignins. *J. Phys. Chem. Lett.* **2011**, *2*, 2846–2852.
- (8) For selected reports of in situ generation of Cu–B species, see: (a) Amenós, L.; Trulli, L.; Nóvoa, L.; Parra, A.; Tortosa, M. Stereospecific Synthesis of α -Hydroxy-Cyclopropylboronates from Allylic Epoxides. *Angew. Chem., Int. Ed.* **2019**, *58*, 3188–3192. (b) Amenós, L.; Nóvoa, L.; Trulli, L.; Arroyo-Bondía, A.; Parra, A.; Tortosa, M. Harnessing the Elusive 1,4-Reduction of Vinyl Epoxides through Copper Catalysis. *ACS Catal.* **2019**, *9*, 6583–6587. For selected reports of in situ generation of Ni–B species, see: (c) Logan, K. M.; Sardini, S. R.; White, S. D.; Brown, M. K. Nickel-Catalyzed Stereoselective Arylboration of Unactivated Alkenes. *J. Am. Chem. Soc.* **2018**, *140*, 159–162. For selected reports of in situ generation of Co–B species, see: (d) Verma, P. K.; Mandal, S.; Geetharani, K. Efficient Synthesis of Aryl Boronates via Cobalt-Catalyzed Borylation of Aryl Chlorides and Bromides. *ACS Catal.* **2018**, *8*, 4049–4054. For selected reports of generation of in situ Fe–B species, see: (e) Zhou, Y.; Wang, H.; Liu, Y.; Zhao, Y.; Zhang, C.; Qu, J. Iron-catalyzed boration of allylic esters: an efficient approach to allylic boronates. *Org. Chem. Front.* **2017**, *4*, 1580–1585.
- (9) For selected reviews, see: (a) Fujihara, T.; Semba, K.; Terao, J.; Tsuji, Y. Regioselective transformation of alkynes catalyzed by a copper hydride or boryl copper species. *Catal. Sci. Technol.* **2014**, *4*, 1699–1709. (b) Semba, K.; Fujihara, T.; Terao, J.; Tsuji, Y. Copper-catalyzed borylative transformations of non-polar carbon-carbon unsaturated compounds employing borylcopper as an active catalyst species. *Tetrahedron* **2015**, *71*, 2183–2197. (c) Sorádová, Z.; Sebesta, R. Enantioselective Cu-Catalyzed Functionalizations of Unactivated Alkenes. *ChemCatChem* **2016**, *8*, 2581–2588. (d) Liu, Y.; Zhang, W. Development of Cu-Catalyzed Asymmetric Addition of Boron to Olefin. *Youji Huaxue* **2016**, *36*, 2249–2271. (e) Chen, J.; Lu, Z. Asymmetric hydrofunctionalization of minimally functionalized alkenes via earth abundant transition metal catalysis. *Org. Chem. Front.* **2018**, *5*, 260–272. (f) Chen, J.; Guo, J.; Lu, Z. Recent Advances in Hydrometallation of Alkenes and Alkynes via the First Row Transition Metal Catalysis. *Chin. J. Chem.* **2018**, *36*, 1075–1109.
- (10) Laitar, D. S.; Tsui, E. Y.; Sadighi, J. P. Catalytic Diboration of Aldehydes via Insertion into the Copper-Boron Bond. *J. Am. Chem. Soc.* **2006**, *128*, 11036–11037.
- (11) Clark et al. subsequently reported Cu-catalyzed diboration of ketones: (a) McIntosh, M. L.; Moore, C. M.; Clark, T. B. Copper-Catalyzed Diboration of Ketones: Facile Synthesis of Tertiary α -Hydroxyboronate Esters. *Org. Lett.* **2010**, *12*, 1996–1999. (b) Moore, C. M.; Medina, C. R.; Cannamela, P. C.; McIntosh, M. L.; Ferber, C. J.; Roering, A. J.; Clark, T. B. Facile Formation of β -Hydroxyboronate Esters by a Cu-Catalyzed Diboration/Matteson Homologation Sequence. *Org. Lett.* **2014**, *16*, 6056–6059.
- (12) Zhao, H.; Dang, L.; Marder, T. B.; Lin, Z. DFT Studies on the Mechanism of the Diboration of Aldehydes Catalyzed by Copper(I) Boryl Complexes. *J. Am. Chem. Soc.* **2008**, *130*, 5586–5594.
- (13) (a) Brook, A. G. Isomerism of Some α -Hydroxysilanes to Silyl Ethers. *J. Am. Chem. Soc.* **1958**, *80*, 1886–1889. (b) Brook, A. G. Molecular Rearrangements of Organosilicon Compounds. *Acc. Chem. Res.* **1974**, *7*, 77–84.

- (14) Recently, Ohmiya et al. developed catalytic transformations involving insertion of aldehyde into the Cu–Si bond and subsequent 1,2-Brook rearrangement: (a) Yabushita, K.; Yuasa, A.; Nagao, K.; Ohmiya, H. Asymmetric Catalysis Using Aromatic Aldehydes as Chiral α -Alkoxyalkyl Anions. *J. Am. Chem. Soc.* **2019**, *141*, 113–117. (b) Takeda, M.; Mitsui, A.; Nagao, K.; Ohmiya, H. Reductive Coupling between Aromatic Aldehydes and Ketones or Imines by Copper Catalysis. *J. Am. Chem. Soc.* **2019**, *141*, 3664–3669. (c) Mitsui, A.; Nagao, K.; Ohmiya, H. Copper-Catalyzed Enantioselective Reductive Cross-Coupling of Aldehydes and Imines. *Org. Lett.* **2020**, *22*, 800–803.
- (15) Molander, G. A.; Wisniewski, S. R. Stereospecific Cross-Coupling of Secondary Organotrifluoroborates: Potassium 1-(Benzyloxy)alkyltrifluoroborates. *J. Am. Chem. Soc.* **2012**, *134*, 16856–16868.
- (16) (a) Kubota, K.; Yamamoto, E.; Ito, H. Copper(I)-Catalyzed Enantioselective Nucleophilic Borylation of Aldehydes: An Efficient Route to Enantiomerically Enriched α -Alkoxyorganoboronate Esters. *J. Am. Chem. Soc.* **2015**, *137*, 420–424. (b) Kubota, K.; Osaki, S.; Jin, M.; Ito, H. Copper(I)-Catalyzed Enantioselective Nucleophilic Borylation of Aliphatic Ketones: Synthesis of Enantioenriched Chiral Tertiary α -Hydroxyboronates. *Angew. Chem., Int. Ed.* **2017**, *56*, 6646–6650.
- (17) For a selected review of β -O elimination, see: (a) Zheng, W.-X.; Zhang, W.-X.; Xi, Z.-F. Cleavage of Chemical Bonds via β -Elimination Reaction of Organometallic Compounds. *Chin. J. Org. Chem.* **2004**, *24*, 1489–1500. For selected examples involving the β -O elimination mechanism, see: (b) Kalsi, D.; Laskar, R. A.; Barsu, N.; Premkumar, J. R.; Sundararaju, B. C-8-Selective Allylation of Quinoline: A Case Study of β -Hydride vs β -Hydroxy Elimination. *Org. Lett.* **2016**, *18*, 4198–4201. (c) Lu, Q.; Greßies, S.; Cembellin, S.; Klauk, F. J. R.; Daniliuc, C. G.; Glorius, F. Redox-Neutral Manganese(I)-Catalyzed C-H Activation: Traceless Directing Group Enabled Regioselective Annulation. *Angew. Chem., Int. Ed.* **2017**, *56*, 12778–12782. (d) Xia, J.; Kong, L.; Zhou, X.; Zheng, G.; Li, X. Access to Substituted Propenoic Acids via Rh(III)-Catalyzed C–H Allylation of (Hetero)-Arenes with Methyleneoxetanones. *Org. Lett.* **2017**, *19*, 5972–5975. (e) Liao, G.; Li, B.; Chen, H.-M.; Yao, Q.-J.; Xia, Y.-N.; Luo, J.; Shi, B.-F. Pd-Catalyzed Atroposelective C-H Allylation through β -O Elimination: Diverse Synthesis of Axially Chiral Biaryls. *Angew. Chem., Int. Ed.* **2018**, *57*, 17151–17155. (f) Kuang, Z.; Chen, H.; Yan, J.; Yang, K.; Lan, Y.; Song, Q. Base-Catalyzed Borylation/B–O Elimination of Propynols and B_2pin_2 Delivering Tetrasubstituted Alkenylboronates. *Org. Lett.* **2018**, *20*, 5153–5157. (g) Wang, Z.; Zhu, L.; Zhong, K.; Qu, L.-B.; Bai, R.; Lan, Y. Mechanistic Insights into Manganese (I)-Catalyzed Chemoselective Hydroarylations of Alkynes: A Theoretical Study. *ChemCatChem* **2018**, *10*, 5280–5286. (h) Zhu, G.; Shi, W.; Gao, H.; Zhou, Z.; Song, H.; Yi, W. Chemodivergent Couplings of *N*-Arylureas and Methyleneoxetanones via Rh(III)-Catalyzed and Solvent-Controlled C–H Activation. *Org. Lett.* **2019**, *21*, 4143–4147.
- (18) For examples of the preparation of cobalt–boryl complexes, see: (a) Adams, C. J.; Baber, R. A.; Batsanov, A. S.; Bramham, G.; Charmant, J. P. H.; Haddow, M. F.; Howard, J. A. K.; Lam, W. H.; Lin, Z.; Marder, T. B.; Norman, N. C.; Orpen, A. G. Synthesis and reactivity of cobalt boryl complexes. *Dalton. Trans.* **2006**, *11*, 1370–1373. (b) Frank, R.; Howell, J.; Campos, J.; Tirfoin, R.; Phillips, N.; Zahn, S.; Mingos, D. M. P.; Aldridge, S. Cobalt Boryl Complexes: Enabling and Exploiting Migratory Insertion in Base-Metal-Mediated Borylation. *Angew. Chem., Int. Ed.* **2015**, *54*, 9586–9590. (c) Rummelt, S. M.; Zhong, H.; Léonard, N. G.; Semproni, S. P.; Chirik, P. J. Oxidative Addition of Dihydrogen, Boron Compounds, and Aryl Halides to a Cobalt(I) Cation Supported by a Strong-Field Pincer Ligand. *Organometallics* **2019**, *38*, 1081–1090.
- (19) For selected examples of cobalt–boryl-catalyzed transformations, see: (a) Obligacion, J. V.; Semproni, S. P.; Chirik, P. J. Cobalt-Catalyzed C–H Borylation. *J. Am. Chem. Soc.* **2014**, *136*, 4133–4136. (b) Yao, W.; Fang, H.; Peng, S.; Wen, H.; Zhang, L.; Hu, A.; Huang, Z. Cobalt-Catalyzed Borylation of Aryl Halides and Pseudohalides. *Organometallics* **2016**, *35*, 1559–1564. (c) Obligacion, J. V.; Semproni, S. P.; Pappas, I.; Chirik, P. J. Cobalt-Catalyzed C(sp²)-H Borylation: Mechanistic Insights Inspire Catalyst Design. *J. Am. Chem. Soc.* **2016**, *138*, 10645–10653. (d) Krautwald, S.; Bezdek, M.; Chirik, P. J. Cobalt-Catalyzed 1,1-Diboration of Terminal Alkynes: Scope, Mechanism, and Synthetic Applications. *J. Am. Chem. Soc.* **2017**, *139*, 3868–3875. (e) Wen, H.; Zhang, L.; Zhu, S.; Liu, G.; Huang, Z. Stereoselective Synthesis of Trisubstituted Alkenes via Cobalt-Catalyzed Double Dehydrogenative Borylations of 1-Alkenes. *ACS Catal.* **2017**, *7*, 6419–6425. (f) Teo, W. J.; Ge, S. Cobalt-Catalyzed Diborylation of 1,1-disubstituted Vinylarenes: A Practical Route to Branched *gem*-Bis(boryl)alkanes. *Angew. Chem., Int. Ed.* **2018**, *57*, 1654–1658. (g) Sang, H. L.; Wu, C.; Phua, G. G. D.; Ge, S. Cobalt-Catalyzed Regiodivergent Stereoselective Hydroboration of 1,3-Dienes To Access Boryl-Functionalized Enynes. *ACS Catal.* **2019**, *9*, 10109–10114.
- (20) For an example of a well-defined PDI–Co–OAr complex, see: Teo, W. J.; Wang, C.; Tan, Y. W.; Ge, S. Cobalt-Catalyzed Z-Selective Hydrosilylation of Terminal Alkynes. *Angew. Chem., Int. Ed.* **2017**, *56*, 4328–4332.